Available online at www.sciencedirect.com

ScienceDirect

journal homepage: www.elsevier.com/locate/he

Hydrogen production by isothermal thermochemical cycles using $La_{0.8}Ca_{0.2}MeO_{3\pm\delta}$ (Me = Co, Ni, Fe and Cu) perovskites

Alejandro Pérez [a], *María Orfila* [a], *María Linares* [a], *Raúl Sanz* [b], *Javier Marugán* [b], *Raúl Molina* [b], *Juan A. Botas* [a,*]

[a] *Department of Chemical, Energy and Mechanical Technology, Rey Juan Carlos University, C/ Tulipán, s/n, Móstoles, 28933, Spain*

[b] *Department of Chemical and Environmental Technology, Rey Juan Carlos University, C/ Tulipán, s/n, Móstoles, 28933, Spain*

HIGHLIGHTS

- $La_{0.8}Ca_{0.2}MeO_{3\pm\delta}$ (Me = Co, Fe, Ni, Cu) can be reduced at 1200, 1000 and 800 °C.
- $La_{0.8}Ca_{0.2}NiO_{3\pm\delta}$ presents a remarkable stability at 800 °C.
- $La_{0.8}Ca_{0.2}NiO_{3\pm\delta}$ can produced 5 $cm^3STP\ H_2/g_{material}$·cycle isothermally at 800 °C.
- $La_{0.8}Ca_{0.2}NiO_{3\pm\delta}$ presents a stable behaviour during 15 consecutive cycles at 800 °C.
- $La_{0.8}Ca_{0.2}NiO_{3\pm\delta}$ thermochemical cycles are compatible with concentrated solar power technologies.

GRAPHICAL ABSTRACT

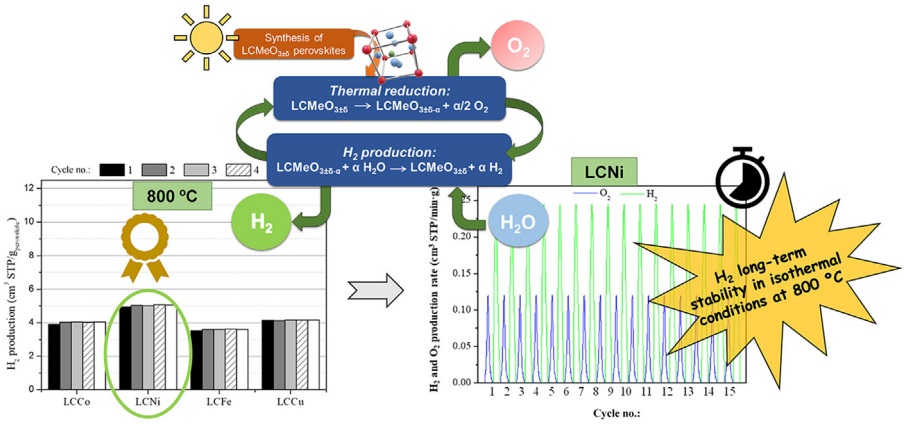

ARTICLE INFO

Article history:
Received 30 October 2022
Received in revised form
14 April 2023
Accepted 24 June 2023
Available online xxx

Keywords:
Thermochemical water splitting
Green hydrogen production

ABSTRACT

Solar-driven thermochemical water splitting has the potential to transform concentrated solar energy into green hydrogen and other solar fuels. In this work, $La_{0.8}Ca_{0.2}MeO_{3\pm\delta}$ (Me = Co, Ni, Fe and Cu) perovskites have been synthesised by a modified Pechini method and evaluated as materials for hydrogen production by two step thermochemical water splitting cycles. Performing the thermal reduction at temperatures of 1200 and 1000 °C, while the oxidation is done at 800 °C, allows a remarkable and stable hydrogen production after 5 consecutive cycles. However, the perovskites suffer changes in the structure after each redox cycle, with potential effects in the long-term cyclic operation. On the contrary, the isothermal thermochemical cycles at 800 °C produce a stable amount of hydrogen with each consecutive cycle maintaining the perovskite structure. This hydrogen production

* *Corresponding author.*
E-mail address: juanangel.botas@urjc.es (J.A. Botas).

https://doi.org/10.1016/j.ijhydene.2023.06.272

Calcium perovskites
Thermodynamic study

ranges from 3.60 cm^3 STP/$g_{material}$·cycle for the material with the lowest productivity ($La_{0.8}Ca_{0.2}FeO_{3\pm\delta}$) to 5.02 cm^3 STP/$g_{material}$·cycle for the one with the highest activity ($La_{0.8}Ca_{0.2}NiO_{3\pm\delta}$). Particularly the Ni-based material shows the highest H_2 productivity accompanied by very good material stability after 15 consecutive cycles, being possible to combine with current solar thermal facilities based on concentrated solar power technologies like plants with central receivers.

Introduction

One of the main concerns of current society is the energy situation marked by fossil fuels dependence and their depletion, the increase of prices, global warming and atmospheric pollution. These facts make it mandatory to look for alternatives that allow meeting the energy needs of today's society without implying a decrease in the quality of life and without harming future generations [1].

It is evident that the solution to these problems must be based on increasing the percentage of energy production from renewable sources. In this context, the Member States of the European Union reached an agreement (June 14th, 2018) so that 32% of the final energy consumed should be of renewable origin by 2030 [2], which implies doubling the current use of renewable energies by EU countries. The main problem is that renewable electrification is not possible in the short to medium term in areas such as the transport sector or thermal applications [3]. Thus, it is necessary to search for alternatives that be technically and economically viable. Among the potential alternatives, the most promising one is the use of hydrogen, as it is an energy vector whose use has no impact on the environment, nor does its production if required energy comes from fully renewable sources [4,5]. Actually, renewable hydrogen is an essential factor in the recently announced recovery instrument of the Next Generation EU, and is recognized as a key solution for i) the decarbonisation of the economy, ii) the elimination of dependence on fossil fuels, iii) the EU's commitment to achieve carbon neutrality by 2050, and iv) the global effort to implement the Paris Agreement [6,7]. It means that the share of hydrogen in Europe's energy mix is projected to grow from the current less than 2% to more than 23% in 2050 for energy uses [8].

Green hydrogen can be obtained by electrolysis of water, using renewable energy as a source of electricity with zero CO_2 emissions. This term is also applied to hydrogen obtained from biogas reforming or biochemical conversion of biomass if sustainability requirements are met during the production [9,10]. Hydrogen can also be obtained from water through thermochemical and photochemical processes, which are less developed than electrolysis, but they also ensure obtaining green hydrogen from water, using renewable energy and with zero CO_2 emissions [11].

Thermochemical production of hydrogen from water involves a series of chemical reactions that convert water into stoichiometric amounts of hydrogen and oxygen using heat as the only energy source. Thermochemical cycles decrease the temperature required for direct water thermolysis (close to 4000 °C), not reachable with existing concentrated solar power technologies. A large number of thermochemical cycles for water splitting has been proposed in the literature, and can be usually grouped into two categories: high-temperature two-steps processes and low-temperature multi-steps processes [12–14]. Low-temperature multi-steps processes, typically with the highest operating temperature below 1000 °C, allow for the use of a broader spectrum of heat sources, such as heat from nuclear power plants, and hence have attracted considerable attention [15]. These cycles suffer from environmental issues associated with the separation of acid mixtures, decomposition of acids, heavy-metal processing, and production of toxic or corrosive intermediates, as most studied cycles are based on Cu–Cl and S–I pairs, which are mediated by the formation of strong acid mixtures of sulphuric, chlorine and/or iodic acids [16–18]. Alternatively, solar-driven thermochemical hydrogen production systems are mainly based on two-steps processes at high-temperature involving the thermal reduction of a metal oxide and its subsequent reoxidation with water, resulting in the dissociation of water in its constituent elements (hydrogen and oxygen) [19–22]. So many different materials have been widely studied in the literature attending to different criteria such as cost, environmental risk, or energy efficiency. However, these materials require high reduction temperatures (>1000 °C) and low oxidation temperatures (~600–800 °C), which imply low energy efficiency of the whole process, as well as several problems due to the high operating temperatures required for the thermal reduction step, such us the stability of solar reactor construction materials, or sintering problems of the metal oxides leading to a lack of long-term stability [12,23]. Considering the above-mentioned problems, it is mandatory to find new materials that can be thermally reduced at lower temperatures without decreasing hydrogen production. In this context non-stoichiometric oxides have been proposed as potential materials for this application as they show a large degree of reduction at moderate temperatures, rapid oxidation and reduction kinetics, favourable oxidation thermodynamics and stability at high temperatures. Particularly perovskites and non-stoichiometric cerium oxide have been proposed as potential materials for this application [24–29].

Perovskite type mixed oxides materials have demonstrated good activity in multiple applications, due to their structure, such as solid fuel cells electrocatalysts or as heterogeneous catalysts [30]. Perovskites are oxides with ABO_3 or A_2BO_4 type structure (A: large cation such as La or Sr; B: smaller cation, such as Mn, Fe, Co, Ni or Cu) that allows the introduction of

Please cite this article as: Pérez A et al., Hydrogen production by isothermal thermochemical cycles using $La_{0.8}Ca_{0.2}MeO_{3\pm\delta}$ (Me = Co, Ni, Fe and Cu) perovskites, International Journal of Hydrogen Energy, https://doi.org/10.1016/j.ijhydene.2023.06.272

different metal ions into its structural framework. Moreover, the cation at both A and B sites could be partially substituted by a foreign one (A′ or B′) without destroying the matrix, allowing the creation of oxygen vacancies or the controlled alteration of the oxidation state of cations to keep the electroneutral state. These changes improve the redox activity of the perovskites due to the presence of oxygen vacancies and the multiple oxidation states of metal in B-position [31–33]. However, despite the temperatures required for the thermal reduction of non-stoichiometric oxides are lower (1000–1300 °C) they are different from the oxidation one (600–800 °C), which decreases the overall thermal efficiency of the global process [34]. The influence of the composition in the temperature required for the thermal reduction of the perovskites is well-known in the field, with perovskites AA'BO_3 able to be reduced at temperatures as low as 400 °C, although with their reoxidation capacity in the presence of water not explored yet [35,36].

In previous studies, the authors have proposed and analysed new materials for H_2 production by solar thermochemical water splitting at reduction temperatures below 900 °C [37,38] and working under isothermal reduction/oxidation conditions (AA'BO_3 perovskites with A = La, A' = Al and B=Co, Ni, Fe, Cu) [39]. Thus, a proper configuration of materials with ABO_3 structure, including selected cations partially substituting the A position occupied by La or Sr, allows obtaining materials with high reduction capacity at temperatures of 800 °C or even 700 °C and oxidizable with water, producing hydrogen under isothermal conditions.

In this work, we focus on Ca as cation for partial substitution of La in $La_{0.8}Ca_{0.2}MeO_{3\pm\delta}$ (Me = Co, Ni, Fe, Cu) perovskites and the application of those materials for hydrogen production by thermochemical water splitting (reactions R1 and R2).

$$La_{0.8}Ca_{0.2}MeO_{3\pm\delta} \rightarrow La_{0.8}Ca_{0.2}MeO_{3\pm\delta-\alpha} + \frac{\alpha}{2}O_2 \quad \text{(R1)}$$

$$La_{0.8}Ca_{0.2}MeO_{3\pm\delta-\alpha} + \alpha H_2O \rightarrow La_{0.8}Ca_{0.2}MeO_{3\pm\delta} + \alpha H_2 \quad \text{(R2)}$$

Calcium has been proposed previously as candidate for partial substitution of $LaCoO_3$ for different applications, including thermochemical water splitting [40–42]. However, thermal reduction of $La_{1-x}Ca_xCoO_3$ ($x \leq 0.4$) has been only evaluated at 1300 °C, although with outstanding results when combined with hydrogen production by oxidation at 900 °C. Ca cation has also been proposed as substitute in perovskites $La_{1-x}Ca_xMnO_{3\pm\delta}$, and tested as effective catalysts in thermochemical solar fuel production, but always at high reduction/oxidation temperatures (1350–1450 °C and 900–1000 °C, respectively), and obtaining a good performance in terms of oxygen exchange capacity and fast oxidation kinetics, but leading to sintering problems in consecutive thermal redox cycles [43]. The partial substitution of La by Ca has been fixed in advance at La/Ca = 0.8/0.2, as it has been demonstrated that ratios higher than 0.6/0.4 lead to segregation of metallic oxides during the synthesis of the perovskite, whereas values of 0.8/0.2 and 0.6/0.4 promote the thermodynamics of the H_2O splitting reaction enhancing the oxidation yields of $La_{1-x}Ca_xCoO_3$ materials, as compared to lower La/Ca substitution ratios [40,41]. Considering the temperatures in which the reduction and oxidation proceed, traditionally the difference between both is accepted as the thermodynamic driving force in the two-step processes [44], due to the consideration of the thermochemical cycle as a closed system. However, the cyclic change between reduction and oxidation temperatures is accompanied by irreversible heat and time losses and creates thermal stresses on the system. Some studies have demonstrated that thermochemical water splitting can be conducted under isothermal conditions by increasing the partial pressure of the steam as compared to the resultant H_2, acting the large partial pressure swing in the gas composition between reduction and oxidation processes as the driving force [45,46]. An increase in the H_2O partial pressure resulted in higher H_2 production capacity, calculated as mass or volume of hydrogen per mass of material and time unit. Consequently, the objective with the $La_{0.8}Ca_{0.2}MeO_{3\pm\delta}$ materials proposed in this work is not only to decrease the reduction temperature to values compatible with current solar thermal facilities, such as those based on solar power tower technologies [47], but also to decrease the gap between reduction and oxidation temperatures, looking for a thermochemical cycle at low temperature and under isothermal conditions. Different studies have demonstrated the feasibility of the thermochemical water and CO_2 splitting mediated by different mixed oxides (perovskites and doped CeO_2) at isothermal conditions with temperatures lower than 1000 °C, even though at lower temperatures the process is controlled by kinetics, reducing the efficiency in terms of hydrogen production [39,48,49].

Materials and methods

Synthesis and characterization of $La_{0.8}Ca_{0.2}MeO_{3-\delta}$ perovskites

All the materials were synthesised following a modified Pechini method described elsewhere using nitrates as metal sources [39]. In a first step, the metal nitrates were mixed in different proportions according to the desired metal composition of each perovskite and incorporated into a citric acid solution in a molar ratio citric acid:metal of 1.5:1. The mixture was stirred at 70 °C for 10 min, acting the citric acid as a chelating agent for metal ions. Then, ethylene glycol was added in a molar ratio citric acid:ethylene glycol of 1:1 to promote the polymerization reaction to transform the chelate obtained with the citric acid into a polymer with a homogeneous distribution of cations. The obtained solution was stirred at 90 °C during 2 h. During this step, ammonium hydroxide was also added until the pH was 8–9, as a basic pH improves the cation distribution [39,50]. After this time, the solution was heated at 130 °C during 4 h, obtaining a viscous gel that was finally washed with water, filtered and dried at 120 °C for 12 h. The obtained resin was milled into a powder form and calcined at 1000 °C for 6 h under static air. Once the different perovskites were obtained, they were analysed using different techniques. First of all, the chemical composition and the oxygen content of the prepared perovskites were obtained using a Varian Vista AX inductively coupled plasma atomic emission spectrometer (ICP-AES), while the crystalline structure was determined by X-ray diffraction (XRD) using a

Please cite this article as: Pérez A et al., Hydrogen production by isothermal thermochemical cycles using $La_{0.8}Ca_{0.2}MeO_{3\pm\delta}$ (Me = Co, Ni, Fe and Cu) perovskites, International Journal of Hydrogen Energy, https://doi.org/10.1016/j.ijhydene.2023.06.272

Philips XPert diffractometer with CuKα radiation. The morphology of the samples was studied by Scanning Electron Microscopy (SEM) using a Hitachi TM1000 microscope with an accelerating voltage of 15 kV and a magnification of ×20~10,000 (2×, 4× digital zoom). Both XRD and SEM techniques were performed before and after the thermochemical cycles. The specific surface area of the samples were measured by N_2 adsorption-desorption at 77 K using a TRISTAR 3000 equipment. The samples were previous degassed at 150 °C for 8 h and the surface area was calculated using the B.E.T. equation. Temperature-programmed reduction under H_2/Ar flow (H_2-TPR) was used to investigate the reducibility of the perovskite materials. The mixed metal oxides were degassed under argon flow (35 NmL/min) for 30 min at 100 °C with a heating rate of 5 °C/min. Afterwards, the H_2-TPR profile was obtained by flowing 10% H_2 in Ar (35 NmL/min) from 100 to 1000 °C with a heating rate of 10 °C/min and, finally, isothermal conditions were maintained for 20 min.

Hydrogen production by thermochemical water splitting

The activity of the materials in terms of hydrogen production by thermochemical water splitting was evaluated in a high temperature tubular furnace coupled to a gas analyser to quantify the amount of oxygen released during the thermal reduction step and the hydrogen produced during the oxidation with water. The details of the reactor configuration have been described elsewhere [51]. In all the experiments, 1 g of material was placed inside the furnace into a Pt/Rh crucible, resistant to the operational temperatures and non-reactive with the metal oxides evaluated in this work. This amount of sample was selected in order to generate a thin layer on the crucible surface, minimizing the diffusional limitations [52]. The thermal reduction step was performed at different temperatures (1200, 1000, 800 °C) to study the influence of the temperature on the stability of the materials and the degree of reduction related to the subsequent hydrogen production. During the reduction reaction, a N_2 flow of 50 NL/h was continuously fed to the furnace to keep an inert environment ($P_{O2} = 10^{-5}$ atm) and to carry out the O_2 released to a paramagnetic gas analyser (Emerson XStream) previously calibrated using nitrogen as zero gas and 0.5% O_2/N_2 as span. A heating rate of 10 °C/min was used until the desired temperature was reached. After that, the temperature was kept constant until oxygen was no longer detected in the analyser.

For the oxidation step, hydrolysis of water, the temperature was decreased to 800 °C with a cooling rate of −10 °C/min, except when the reduction was also performed at 800 °C. After that, a nitrogen flow of 50 NL/h saturated in water vapour at 80 °C was continuously fed to the furnace ($P_{H2O} = 7.2 \cdot 10^{-4}$ atm). The resulting gas mixture from the reactor passed through a moisture trap followed by a cooling step to 3 °C to condensate traces of unreacted water before the hydrogen analyser (Emerson XStream equipped with a thermal conductivity detector). The analyser was previously calibrated using nitrogen as zero gas and 0.5% H_2/N_2 as span. The temperature was kept at 800 °C until hydrogen was no longer detected in the analyser.

The reduction and oxidation temperatures were selected according to a preliminary theoretical evaluation of the evolution of Gibbs free energy, ΔG_r^T, with the temperature, for both reactions (R1 and R2). ΔG_r^T was calculated from the standard enthalpies and entropies of formation (ΔH_f^0 and ΔS_f^0) and the temperature dependence of the specific heat of the species ($C_p(T)$) according to the procedure described elsewhere [51] and applied to reactions R1 and R2. The thermodynamic data of the perovskites have been estimated using the Neumann-Kopp rule (NKR) for mixed oxides [53] combined with vacant model calculations [54]. The properties of pure metal oxides, hydrogen, oxygen and water were obtained from the HSC Chemistry 6.0 software from ©Outotec Research Oy.

Results

Perovskites characterization

ICP-AES measurements were performed to determine the elemental analysis and the atomic ratio (La/Ca/Me) of the different synthesised materials. Additionally, it is possible to calculate the oxygen composition of the materials and the non-stoichiometry (defect or excess) of oxygen (δ) by performing a mass balance between the total mass used for ICP analysis and the amount of each metal present in the sample. The difference between the calculated and the theoretical oxygen stoichiometry (3) corresponds to δ. As it can be seen in the results summarized in Table 1, all the materials show a metallic composition close to the theoretical one, confirming that the syntheses were successful. All the materials present a degree of non-stoichiometry (excess or defect), with values ranging from −0.04 to +0.02 for the mean compositions.

This oxygen non-stoichiometry is due to the partial lanthanum substitution by calcium. When some of the La^{3+} cations are replaced by Ca^{2+} the same number of atoms of Me^{3+}/Me^{2+} is oxidized to Me^{4+}/Me^{3+} in order to maintain the electroneutrality of the materials. These new cations are not stable enough and they tend to partially reduce themselves. These processes inside the perovskite lattice improve the formation of non-stoichiometric oxygen [55,56].

Once the samples were analysed by ICP they were also characterised by XRD to study their crystal structure. Fig. 1

Table 1 – Composition of the synthesised perovskites $La_{0.8}Ca_{0.2}MeO_{3\pm\delta}$.

Perovskite	Label	La	Ca	Me = Co/Ni/Fe/Cu	δ
$La_{0.8}Ca_{0.2}CoO_{3\pm\delta}$	LCCo	0.83 ± 0.037	0.19 ± 0.015	1 ± 0.09	−0.04
$La_{0.8}Ca_{0.2}NiO_{3\pm\delta}$	LCNi	0.84 ± 0.013	0.23 ± 0.008	1 ± 0.07	−0.02
$La_{0.8}Ca_{0.2}FeO_{3\pm\delta}$	LCFe	0.81 ± 0.026	0.21 ± 0.017	1 ± 0.01	+0.02
$La_{0.8}Ca_{0.2}CuO_{3\pm\delta}$	LCCu	0.79 ± 0.02	0.18 ± 0.019	1 ± 0.012	−0.01

Please cite this article as: Pérez A et al., Hydrogen production by isothermal thermochemical cycles using $La_{0.8}Ca_{0.2}MeO_{3\pm\delta}$ (Me = Co, Ni, Fe and Cu) perovskites, International Journal of Hydrogen Energy, https://doi.org/10.1016/j.ijhydene.2023.06.272

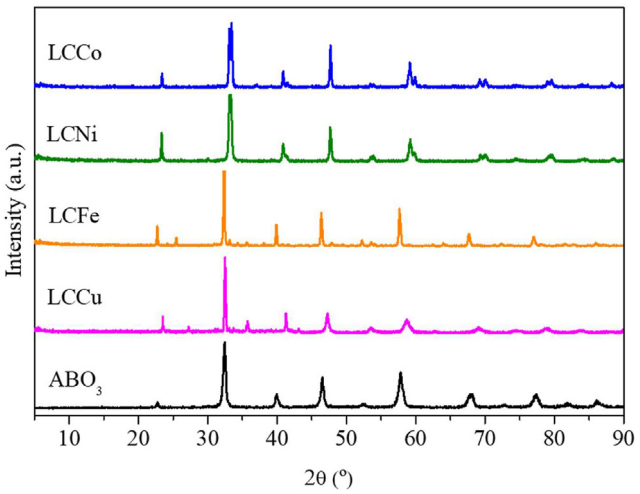

Fig. 1 – XRD patterns for the $La_{0.8}Ca_{0.2}MeO_{3\pm\delta}$ materials.

shows XRD diffractions for all the materials, as compared to the reference ABO_3 pattern. The results showed a single perovskite phase for all the materials with small contributions of other crystal phases in the case of Cu perovskite, assigned to CuO (35°) [57]. Table 2 shows the lattice parameters obtained from Rietveld refinement, demonstrating that Co, Ni and Fe perovskites showed a cubic structure (Pm3m-221) while Cu perovskite presented a tetragonal one (P4/mmm-123). The shift to a higher angle for Co- and Ni-based materials indicates the insertion of a smaller B atom into the crystal lattice. The effect is less remarkable in the case of Cu, due to the basic pH during the synthesis [39]. The different structure of LCCu as compared to the other perovskites can be due to the different oxidation states of the metals in B position, leading those with charge 3+ or 4+ (Co, Fe, Ni) to lower distortions in the structure than that with 2+ charge (Cu).

Table 2 also shows the Goldschmidt's tolerance factor (t) calculated for all the perovskites as described elsewhere [39]. This parameter is also a measure of the distortion produced in the perovskite due to the partial substitution of La by Ca (obtaining $AA'BO_3$ instead ABO_3 perovskite). This parameter should be in the range of $0.75 < t < 1$. A value of $t = 1$ is attributed to the perfect cubic ABO_3 perovskite structure, and values far from 1 are characteristics of other perovskites structures, such as orthorhombic or tetragonal structures.

The surface morphology of the LCMe (Me = Co, Ni, Fe, Cu) perovskites was observed by scanning electron microscopy (SEM). As shown in Fig. 2, an irregular porous structure arranged with many small particles was observed for all the materials. Similar surface structures were observed in other LCCo-based perovskites [41]. This porous structure can enhance the gas-solid reactions during the reduction/oxidation processes, promoting a faster reactants and products transportation and overall reaction kinetics.

The specific surface area (S_{BET}) of the synthesised materials was analysed by N_2 adsorption-desorption, and the obtained results are summarized in Table 3.

The low S_{BET} obtained for all the materials are characteristics of similar mixed oxides structures reported in the literature [58], ranging from 3.45 m^2/g for the material with the lowest surface (LCFe) to 8.89 m^2/g for the material with the highest surface (LCCo).

Finally, temperature programmed reduction (TPR) was used to evaluate the reducibility of the materials. Fig. 3 shows H_2-TPR profiles of the LCMe synthesised perovskites.

All the materials present several reduction signals except for LCCu perovskite. First of all, it should be noticed that the shoulder peaks presented in all the perovskites at temperatures between 250 and 300 °C are due to the removal of non-stoichiometry oxygen (O_δ) and some other weakly bonded oxygen in the perovskite network [59]. In the case of the LCCo material the small signal at 319.5 °C could be attributed to the reduction of Co^{4+}, which is very unstable, while the peak located at 412 °C could be attributed to the reduction of Co^{3+}. Finally, the signals located at 814.3 and 978.6 °C are due to the reduction of Co^{2+} [60]. Regarding the LCNi perovskite, the signal located at 337.2 °C could be due to the reduction of Ni^{3+} to Ni^{2+}, while the signals at 581 °C and 798.5 °C are due to the reduction of Ni^{2+} to Ni^0, outer and inner ions, respectively [59]. Concerning the LCFe material the signal located at 423.6 °C could be due to the reduction of Fe^{4+} to Fe^{3+}. Fe^{4+} ions appear in order to maintain the electroneutrality of the material due to the partial substitution of La^{3+} by Ca^{2+}. On the other hand, the peak located at 557.6 °C is due to the reduction of Fe^{3+}, while last signals are attributable to outer and inner Fe^{2+} [52]. Finally, the perovskite with Cu in B position showed a completely different profile. In this case, the first peak could be due to the reduction of Cu^{2+} to Cu^0 which occurs at very low temperatures [61].

Evaluation of the hydrogen production activity

The temperature required for the thermal reduction of the metal oxide (reaction R1) is a critical factor that hinders the application of the materials for hydrogen production by thermochemical water splitting. Additionally, the gap in the reduction and oxidation temperatures induces irreversible

Table 2 – Goldschmidt's tolerance factor (t) and crystal structural values of synthesised $La_{0.8}Ca_{0.2}MeO_{3\pm\delta}$ perovskites obtained from Rietveld refinement.

Material	t	Crystal structure	a (Å)	b (Å)	c (Å)	V (Å^3)
Reference Pm3m-221	-	Cubic	3.903	3.903	3.903	59.456
Reference P4/mmm-123	-	Tetragonal	3.786	3.786	11.386	163.25
LCCo	0.899	Cubic	3.826	3.826	3.826	56.008
LCNi	0.914	Cubic	3.824	3.824	3.824	55.942
LCFe	0.838	Cubic	3.907	3.907	3.907	59.659
LCCu	0.805	Tetragonal	3.806	3.806	11.51	166.75

Please cite this article as: Pérez A et al., Hydrogen production by isothermal thermochemical cycles using $La_{0.8}Ca_{0.2}MeO_{3\pm\delta}$ (Me = Co, Ni, Fe and Cu) perovskites, International Journal of Hydrogen Energy, https://doi.org/10.1016/j.ijhydene.2023.06.272

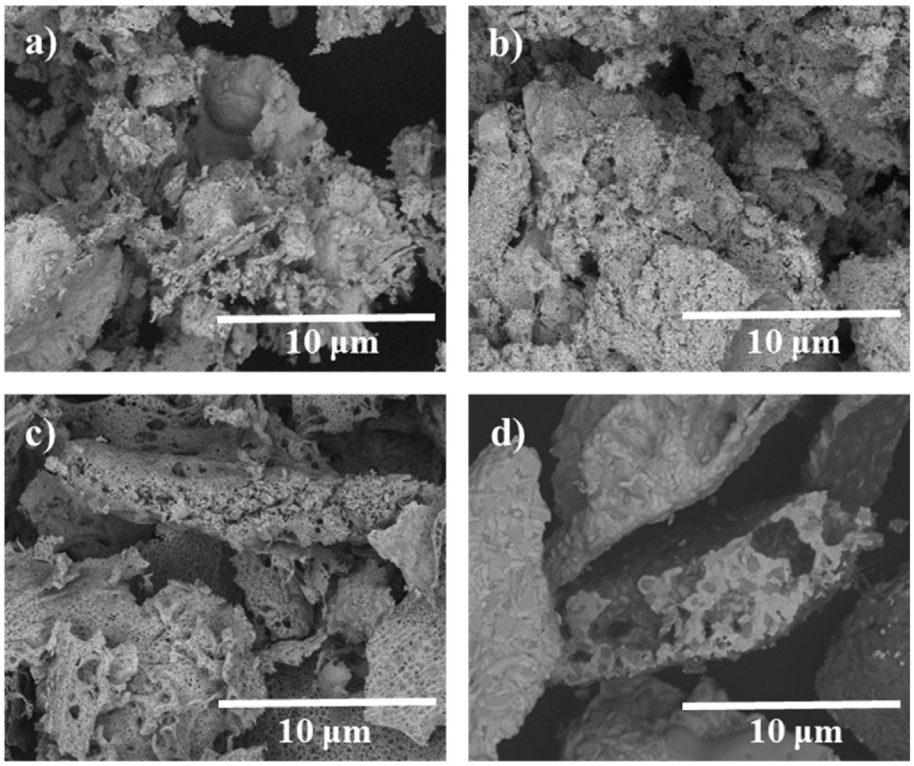

Fig. 2 – SEM micrographs of the LCMe materials: a) LCCo, b) LCNi, c) LCFe and d) LCCu.

Table 3 – Specific surface area (S_{BET}) of the synthesised $La_{0.8}Ca_{0.2}MeO_{3\pm\delta}$ perovskites.

Material	S_{BET} (m^2/g)
LCCo	8.89
LCNi	7.67
LCFe	3.45
LCCu	4.38

heat losses and creates thermal stresses on the system. Thus, for a first approximation to the temperatures of the process, a theoretical evaluation of the evolution of Gibbs free energy with temperature for the thermal reduction was performed for all the materials, assuming an extent of the reaction $0.25 \leq \alpha \leq 1$. Table 4 shows temperatures for $\Delta G_r^T = 0$, at different values of α (complete results are shown as supplementary information).

Depending on the extent of the reaction, temperatures ranging between 700 °C and 1100 °C are necessary to promote the thermal reduction of the La–Ca-based perovskites under study. It should be remarked that these results are at thermodynamic equilibrium, and they do not take into account the influence of temperature in kinetics or the continuous removal of the oxygen released in a further experimental reactor [51,62,63]. Consequently, and also taking into account other works related to isothermal (low temperature) thermochemical water splitting systems, a range of reduction temperatures from 1200 to 800 °C, and an oxidation temperature of 800 °C were fixed for the experimental study (considering the isothermal conditions at 800 °C, close to the temperature suggested in other studies for this process of water splitting) [48,49].

Fig. 4 shows the hydrogen production after five consecutive cycles (a) and the XRD diffractions (b) of all the materials before and after the cycles, using a reduction temperature of 1200 °C. LCNi and LCFe show stable production of 11 and 9.4 H_2 cm^3 STP/$g_{perovskite}$ in each consecutive cycle, respectively. LCCo and LCCu show a slight decrease in the activity after each cycle, higher in the case of the LCCo. In all cases, the obtained H_2/O_2 molar ratio was 1.97 ± 0.02, close to the theoretical value of 2 for water splitting to H_2 and O_2 according to reaction R3.

$$H_2O \rightarrow H_2 + \frac{1}{2}O_2 \quad \text{(R3)}$$

There are several differences between XRD spectra of materials after activity cycles and the corresponding to the starting materials (except for the LCFe), mainly due to changes in the perovskite crystal structure and the appearance of new crystal phases. The structure of the LCCo material changes from cubic to tetragonal, with signals of segregated phases of pure metal oxides attributed to Co_3O_4 and CoO. Similar behaviour exhibits the LCNi, with segregation of NiO_x and NiO after the thermochemical cycles at reduction temperature of 1200 °C [64]. In the case of LCCu, it retains its tetragonal structure, but the signals attributed to segregation of CuO become more relevant, evidencing the poor stability of the material, although that obtained after each cycle also seems active. The lower stability of this material could be explained by the different oxidation states of this metal. As some of the La^{3+} ions have been replaced by Ca^{2+} ions, it is necessary to maintain the electroneutrality,

Please cite this article as: Pérez A et al., Hydrogen production by isothermal thermochemical cycles using $La_{0.8}Ca_{0.2}MeO_{3\pm\delta}$ (Me = Co, Ni, Fe and Cu) perovskites, International Journal of Hydrogen Energy, https://doi.org/10.1016/j.ijhydene.2023.06.272

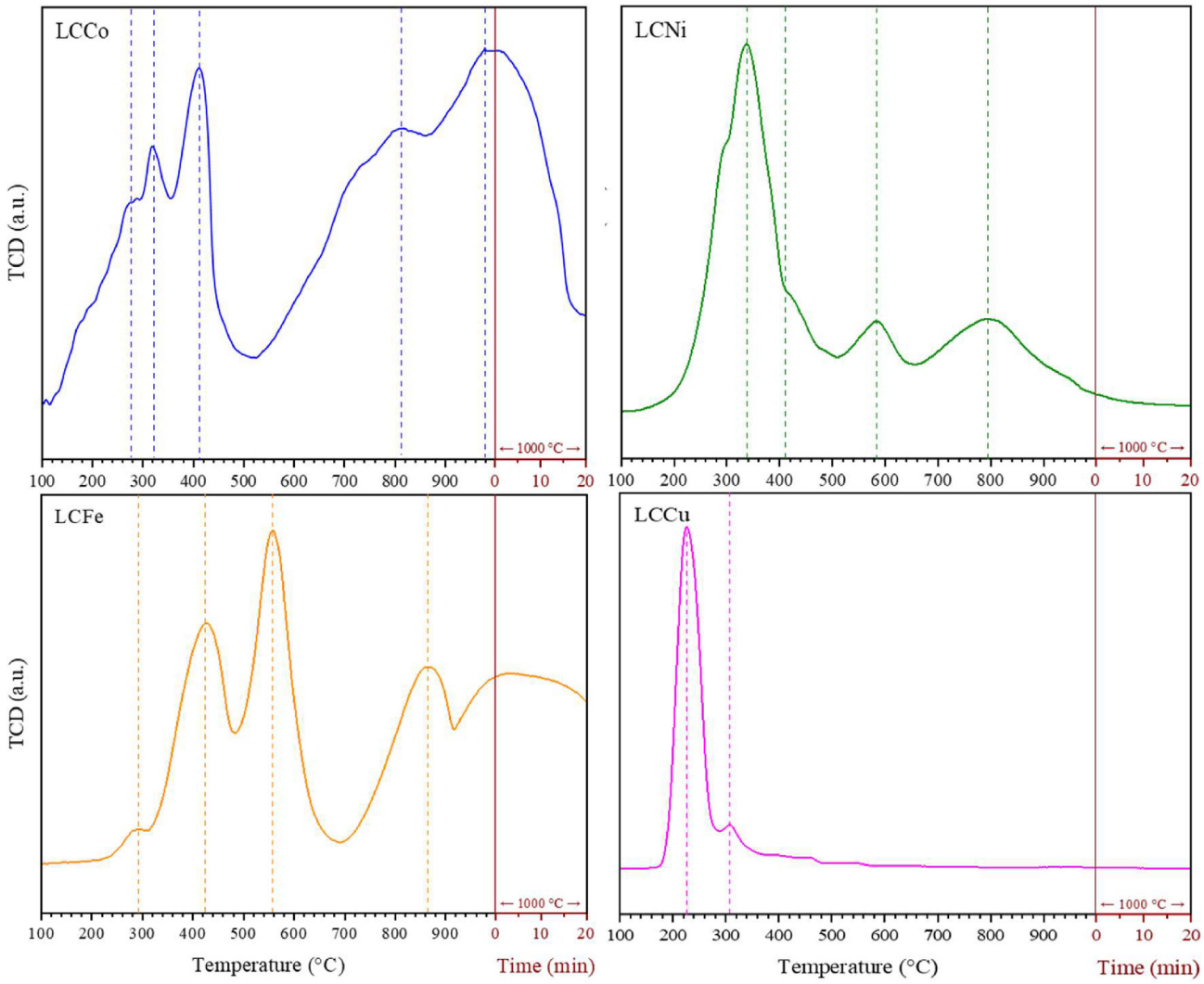

Fig. 3 – H_2-TPR profiles of the synthesised perovskites: LCCo, LCNi, LCFe and LCCu.

Table 4 – Theoretical temperature necessary for $\Delta G_r^T = 0$ in thermal reduction step of LCMe materials.

Extent of reaction	LCCo	LCNi	LCFe	LCCu
$\alpha = 0.25$	700 °C	725 °C	700 °C	800 °C
$\alpha = 0.5$	710 °C	825 °C	710 °C	825 °C
$\alpha = 1$	775 °C	1100 °C	775 °C	890 °C

and thus, the metal in B position should have higher oxidation state. Due to this, if Cu^{2+} is reduced to Cu^{+} during thermal reduction, it implies lower stability of the resultant material because of the difficulty of maintaining global electroneutrality [65]. Additionally, the samples after cycles were also analysed by SEM and the micrographs are shown in Fig. S3, confirming the presence of new segregated phases at high temperatures. It should be remarked that those changes in the materials could affect the activity of the perovskites in the long-time, even though the activity is not affected after only 5 cycles (case of LCNi and LCFe), hindering the application of the materials at least under the proposed thermal conditions.

The decrease of the reduction temperature from 1200 °C to 1000 °C also produces a decrease in hydrogen production in all cases (Fig. 5a), although it is stable during the cycles. The H_2/O_2 molar ratio was also 2.02 ± 0.02, corresponding to the complete water splitting (reaction R3). However, the distortion in the LCMe structures is still noticeable except for the Fe-based material (Fig. 5b). In LCCo, there are small changes in the signals due to the presence of orthorhombic perovskite crystal phase (Pnma-61) after reduction/oxidation at 1000/800 °C. Regarding the LCNi perovskite, there are new arising signals due to the presence of NiO, while the main perovskite still maintains its cubic structure. Concerning the LCCu perovskite, it remains a tetragonal crystal phase (P4/mmm-123), with presence of CuO but in less extension than the sample after performing the redox cycles at 1200/800 °C.

Finally, performing the thermochemical water splitting under isothermal conditions at 800 °C implies a decrease in hydrogen production, although materials maintain their structure completely after the cycles (Fig. 6). It is remarkable that the behaviour of the materials changes at these conditions. Thus, LCCo is not the most active perovskite, being

Please cite this article as: Pérez A et al., Hydrogen production by isothermal thermochemical cycles using $La_{0.8}Ca_{0.2}MeO_{3\pm\delta}$ (Me = Co, Ni, Fe and Cu) perovskites, International Journal of Hydrogen Energy, https://doi.org/10.1016/j.ijhydene.2023.06.272

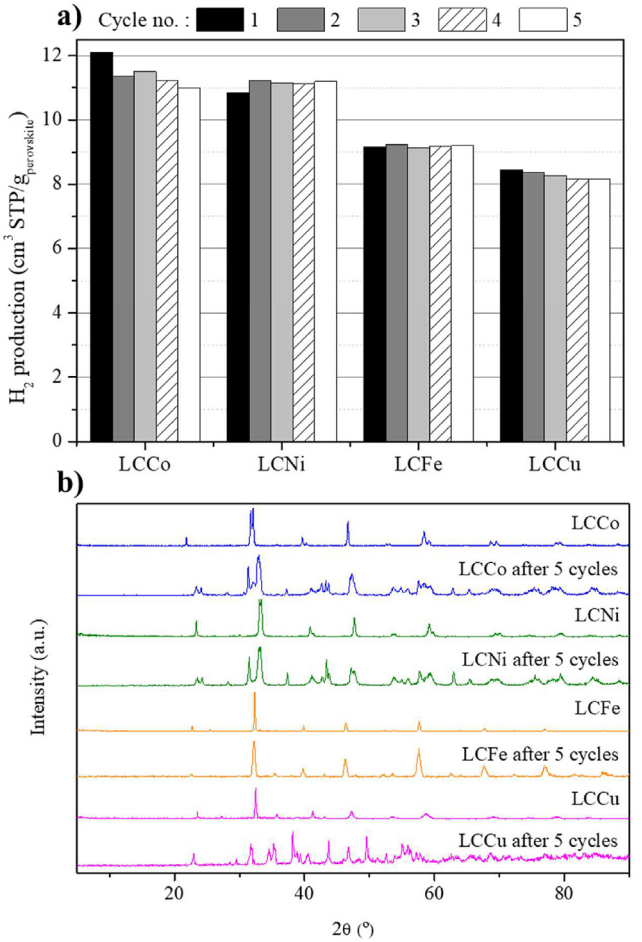

Fig. 4 – a) Hydrogen production and b) XRD before and after 5 consecutive cycles of thermochemical water splitting at reduction and oxidation temperatures of 1200 and 800 °C, respectively.

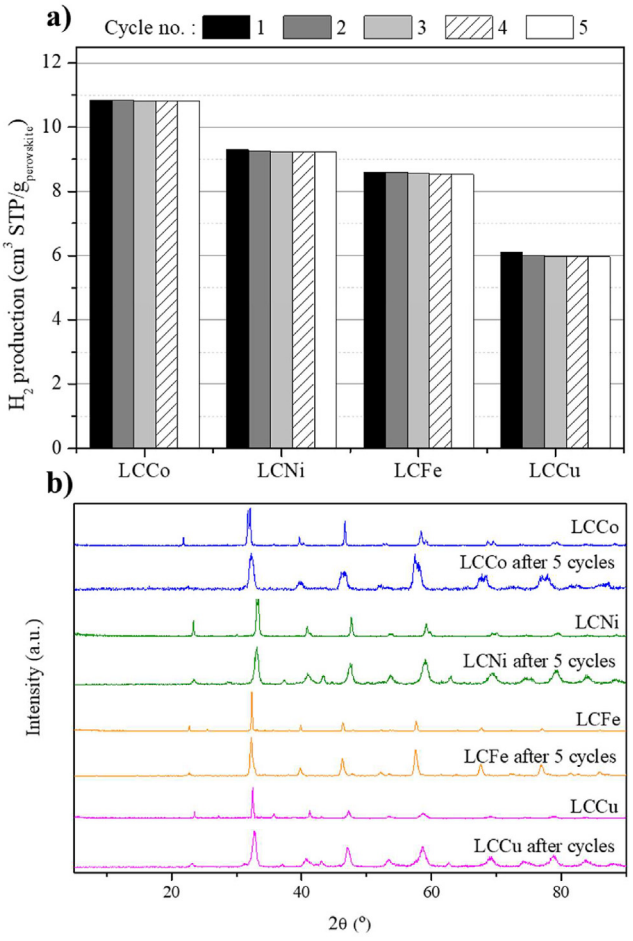

Fig. 5 – a) Hydrogen production and b) XRD before and after 5 consecutive cycles of thermochemical water splitting at reduction and oxidation temperatures of 1000 and 800 °C, respectively.

overcome by the LCNi (5.02 vs. 4.01 H_2 cm^3 STP/$g_{perovskite}$ per cycle, respectively). Even production with LCCu exceeds that obtained by LCFe (4.14 and 3.60 H_2 cm^3 STP/$g_{perovskite}$ per cycle, respectively). This fact is related to the reducibility observed by the materials in the TPR analysis (Fig. 3). From those results, the four perovskites could lose some of their reduction capacity at 800 °C, being this effect in a higher degree for materials LCCo and LCFe. In all cases, the H_2/O_2 molar ratio was 2.00 ± 0.07, corresponding to the theoretical stoichiometry of water splitting to hydrogen and oxygen (reaction R3).

Cyclic operation under isothermal conditions at higher temperatures (for example 1000 °C) could be a possibility to increase the reduction extent, and consequently the further hydrogen production during the subsequent oxidation (hydrolysis) at the same temperature. However, it has been demonstrated that the solar to hydrogen efficiency of the isothermal systems is lower than thermochemical cycles working with $T_{reduction} > T_{oxidation}$ in the range of temperatures usually employed for thermal reduction of perovskites or cerium oxide based materials (>1100 °C) due to water splitting thermodynamics [12,66]. The theoretical evaluation of the evolution of the Gibbs free energy of the oxidation with water (see supplementary information) shows that 800 °C is in the limit to obtain a $\Delta G_r^T = 0$, and higher temperatures clearly make positive that reaction parameter, making difficult the spontaneity of the reaction. To check this hypothesis, the isothermal water splitting with the LCNi perovskite was performed at 1000 °C (not shown). Besides the distortion in the material obtained after the redox cycle, the hydrogen production hardly reached 5.99 ± 1.8 H_2 cm^3 STP/$g_{perovskite}$·cycle, as compared to the results obtained with a swift of temperatures between 1000 and 800 °C (9.25 ± 0.03 H_2 cm^3 STP/$g_{perovskite}$·cycle, Fig. 5) or even under isothermal conditions at 800 °C (5.02 ± 0.07 H_2 cm^3 STP/$g_{perovskite}$·cycle, Fig. 6), but reducing 200 °C the maximum temperature required for the process.

Considering all the previous results, isothermal conditions at 800 °C seem a good option to obtain a remarkable activity maintaining the structure of the materials over the cycles. However, in addition to the overall hydrogen production in each cycle, an interesting parameter is the hydrogen average production rate. Each material has different total hydrogen production per cycle but also different oxidation times to reach the maximum extent of the oxidation in each cycle.

Please cite this article as: Pérez A et al., Hydrogen production by isothermal thermochemical cycles using $La_{0.8}Ca_{0.2}MeO_{3\pm\delta}$ (Me = Co, Ni, Fe and Cu) perovskites, International Journal of Hydrogen Energy, https://doi.org/10.1016/j.ijhydene.2023.06.272

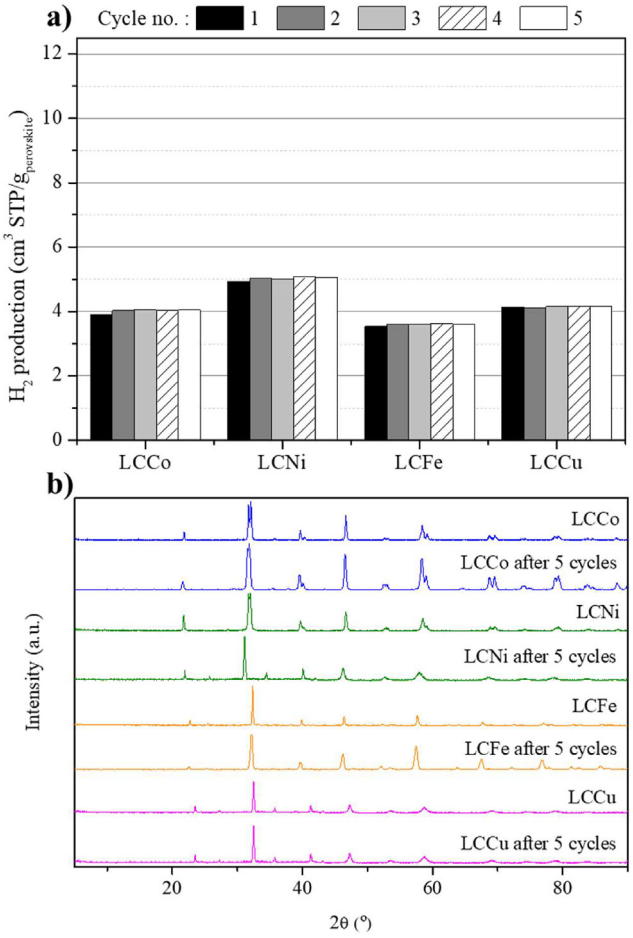

Fig. 6 – a) Hydrogen production and b) XRD before and after 5 consecutive cycles of thermochemical water splitting at isothermal conditions (800 °C).

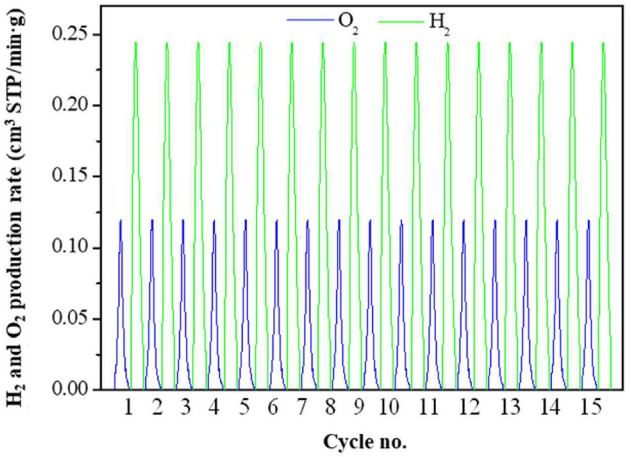

Fig. 7 – Hydrogen and Oxygen production rate using LCNi in 15 consecutive isothermal thermochemical cycles at 800 °C.

Consequently, comparison of hydrogen average production rates could be used to check the most productive material to maximize hydrogen production in a further up-scale application. Table 5 shows the data of H_2 and O_2 productions and average production rates per cycle for the isothermal thermochemical cycles at 800 °C with the synthesised perovskites. The average production rates are calculated as the H_2 and O_2 production data divided by the total time required by the perovskite oxidation or reduction steps, respectively.

The hydrogen average production rate follows a different behaviour for each material, being 0.080, 0.070, 0.067 and 0.062 H_2 cm^3 STP/$g_{perovskite}$·min for LCNi, LCCu, LCCo and LCFe, respectively. The oxygen average production rate was also calculated, reaching values of 0.033, 0.030, 0.027 and 0.026 O_2 cm^3 STP/$g_{perovskite}$·min for LCNi, LCCu, LCCo and LCFe, respectively, confirming the LCNi material as the most promising one for the isothermal thermochemical water splitting at 800 °C. In view of these results, the activity of this perovskite was tested during 15 consecutive cycles showing a very good reproducibility (Fig. 7).

Although the production is lower than that reported in the literature for other isothermal water splitting processes, such as that based on hercynite, it should be emphasized that commonly isothermal processes are based on reduction/oxidation temperatures higher than 1000 °C, instead of 800 °C tested in this work [45].

Conclusions

Partial substitution of La^{3+} ions by Ca^{2+} ions in the $LaMeO_3$ (Me = Co, Ni, Fe and Cu) perovskites allows obtaining materials with remarkable redox properties to be used for hydrogen production by thermochemical water splitting. LCMe materials can be thermally reduced in a range of temperatures from 1000 to 800 °C, maintaining a remarkable hydrogen production even under isothermal conditions of 800 °C. At those conditions, the structure of the materials remain unaltered after the thermochemical cycles, without hindering their performance in the long-term operation. Particularly, the LCNi material ($La_{0.8}Ca_{0.2}NiO_{3\pm\delta}$) has proven a stable behaviour in terms of hydrogen production during 15 consecutive cycles.

Table 5 – H_2 and O_2 productions and average production rates at 800 °C.

	Production (cm^3 STP/$g_{perovskite}$·cycle)		Average production rate (cm^3 STP/$g_{perovskite}$·min)	
	H_2	O_2	H_2	O_2
LCCo	4.01 ± 0.024	1.93 ± 0.034	$0.067 \pm 4 \cdot 10^{-4}$	$0.027 \pm 5 \cdot 10^{-4}$
LCNi	5.02 ± 0.038	2.43 ± 0.032	$0.080 \pm 6 \cdot 10^{-4}$	$0.033 \pm 4.6 \cdot 10^{-4}$
LCFe	3.60 ± 0.022	1.79 ± 0.016	$0.062 \pm 3.6 \cdot 10^{-4}$	$0.026 \pm 2.2 \cdot 10^{-4}$
LCCu	4.14 ± 0.014	2.06 ± 0.017	$0.070 \pm 2.3 \cdot 10^{-4}$	$0.030 \pm 2.4 \cdot 10^{-4}$

Please cite this article as: Pérez A et al., Hydrogen production by isothermal thermochemical cycles using $La_{0.8}Ca_{0.2}MeO_{3\pm\delta}$ (Me = Co, Ni, Fe and Cu) perovskites, International Journal of Hydrogen Energy, https://doi.org/10.1016/j.ijhydene.2023.06.272

These results are critical for the commercial viability of solar thermochemical active materials. Moreover, the low temperature required for this material as compared to common two-step thermochemical cycles working at different reduction/oxidation temperatures (cerium oxide) or under isothermal conditions (hercynite) could be a solution to the variability of the hydrogen production that could be expected in solar reactors due to drastic changes in those systems that occur with cloud coverage, for example. The results demonstrate the potential interest of this material to produce hydrogen under isothermal conditions at a temperature as low as 800 °C, being possible to combine this system with current solar thermal facilities based on concentrated solar power technologies like plants with central receivers.

Declaration of competing interest

The authors declare that they have no known competing financial interests or personal relationships that could have appeared to influence the work reported in this paper.

Acknowledgements

The authors wish to thank "Comunidad de Madrid" and European Structural Funds for their financial support to ACES2030-CM (S2018/EMT-4319) project and ONEHYDRO (M – 2733) URJC project.

Appendix A. Supplementary data

Supplementary data to this article can be found online at https://doi.org/10.1016/j.ijhydene.2023.06.272.

REFERENCES

[1] International Energy Agency. "Global energy review 2021". Global Energy Review 2022:1–36. 2021.
[2] EU. Directive (EU) 2018/2001 of the European Parliament and of the Council of 11 December 2018 on the promotion of the use of energy from renewable sources (recast). Off J Eur Union 2018;2018(L 328):82–209.
[3] Ministerio para la Transición Ecológica y el Reto Demográfico (MITERD). Hoja de Ruta del Hidrógeno. Una apuesta por el hidrógeno renovable. 2013.
[4] Nikolaidis P, Poullikkas A. A comparative overview of hydrogen production processes. Renewable Sustainable Energy Rev 2017;67:597–611. https://doi.org/10.1016/j.rser.2016.09.044.
[5] Gopinath M, Marimuthu R. A review on solar energy-based indirect water-splitting methods for hydrogen generation. Int J Hydrogen Energy 2022;47(89):37742–59. https://doi.org/10.1016/j.ijhydene.2022.08.297.
[6] Comission E. Communication from the commission to the European parliament, the council, the European economic and social committee and the committee of the regions: a hydrogen strategy for a climate-neutral Europe. COM 2020;301:2020.
[7] Comission E. Communication from the commission to the European parliament, the council, the European economic and social committee and the committee of the regions. The European Green Deal. COM 2019;640:2019.
[8] Centre JR. Hydrogen use in EU decarbonization scenarios. 2019.
[9] Safari F, Dincer I. A review and comparative evaluation of thermochemical water splitting cycles for hydrogen production. Energy Convers Manag 2020;205:112182. https://doi.org/10.1016/j.enconman.2019.112182. article number.
[10] Zhang F, Zhao P, Niu M, Maddy J. The survey of key technologies in hydrogen energy storage. Int J Hydrogen Energy 2016;41(33):14535–52. https://doi.org/10.1016/j.ijhydene.2016.05.293.
[11] da Silva Veras T, Mozer TS, da Costa Rubim Messeder dos Santos D, da Silva César A. Hydrogen: trends, production and characterization of the main process worldwide. Int J Hydrogen Energy 2017;42(4):2018–33. https://doi.org/10.1016/j.ijhydene.2016.08.219.
[12] Rao CNR, Dey S. Solar thermochemical splitting of water to generate hydrogen. P.N.A.S. 2017;114(51):13385–93. https://doi.org/10.1073/pnas.1700104114.
[13] Kodama T, Gokon N. Thermochemical cycles for high-temperature solar hydrogen production. Chem Rev 2007;107(10):4048–77. https://doi.org/10.1021/cr050188a.
[14] Boretti A. Which thermochemical water-splitting cycle is more suitable for high-temperature concentrated solar energy? Int J Hydrogen Energy 2022;47(1):20462–74. https://doi.org/10.1016/j.ijhydene.2022.04.159.
[15] Li X, Sun X, Song Q, Yang Z, Wang H, Duan Y. A critical review on integrated system design of solar thermochemical water-splitting cycle for hydrogen production. Int J Hydrogen Energy 2022;47(79):33619–42. https://doi.org/10.1016/j.ijhydene.2022.07.249.
[16] Singh RV, Pai MR, Banerjee AM, Nayak C, Phapale S, Bhattacharvya D, Tripathi AK. Cu–Cl thermochemical water splitting cycle: probing temperature-dependent $CuCl_2$ hydrolysis and thermolysis reaction using in situ XAS. J Therm Anal Calorim 2022;147(12):7063–76. https://doi.org/10.1007/s10973-021-10969-y.
[17] Russ B, Buckingham R, Brown L, Moore R, Helie M, Carle P, Pons N, Ode D, Duhamet J, Leybros J. Summary of the sulfur-iodine process integrated laboratory-scale experiment. Nucl Technol 2012;178(1):94–110. https://doi.org/10.13182/NT12-A13550.
[18] Osuolale F, Ogunleye O, Fakunle M, Busari A, Abolanle Y. Comparative studies of Cu-Cl thermochemical water decomposition cyles for hydrogen production. E3S Web Conf 2018;61:00009. https://doi.org/10.1051/e3sconf/20186100009. article number.
[19] Yilmaz F, Balta MT, Selbaş R. A review of solar based hydrogen production methods. Renewable Sustainable Energy Rev 2016;56:171–8. https://doi.org/10.1016/j.rser.2015.11.060.
[20] Charvin P, Stéphane A, Florent L, Gilles F. Analysis of solar chemical processes for hydrogen production from water splitting thermochemical cycles. Energy Convers Manag Jun. 2008;49(6):1547–56. https://doi.org/10.1016/j.enconman.2007.12.011.
[21] Mao Y, Gao Y, Dong W, Wu H, Song Z, Zhao X, Sun J, Wang W. Hydrogen production via a two-step water splitting thermochemical cycle based on metal oxide – a review. Appl Energy 2020;267:114860. https://doi.org/10.1016/j.apenergy.2020.114860. article number.
[22] Lee S, Na UJ, Jo H. Techno-economic assessment of green hydrogen production via two-step thermochemical water splitting using microwave. Int J Hydrogen Energy 2023;48(29):10706–23. https://doi.org/10.1016/j.ijhydene.2022.12.119.

Please cite this article as: Pérez A et al., Hydrogen production by isothermal thermochemical cycles using $La_{0.8}Ca_{0.2}MeO_{3\pm\delta}$ (Me = Co, Ni, Fe and Cu) perovskites, International Journal of Hydrogen Energy, https://doi.org/10.1016/j.ijhydene.2023.06.272

[23] Abanades S. Metal oxides applied to thermochemical water-splitting for hydrogen production using concentrated solar energy. Chem Eng 2019;3(3). https://doi.org/10.3390/chemengineering3030063.
[24] Şanlı SB, Pişkin B. Effect of B-site Al substitution on hydrogen production of $La_{0.4}Sr_{0.6}Mn_{1-x}Al_x$ (x=0.4, 0.5 and 0.6) perovskite oxides. Int J Hydrogen Energy 2022;47(45):19411–21. https://doi.org/10.1016/j.ijhydene.2021.12.047.
[25] Bhosale RR, Takalkar G, Sutar P, Kumar A, AlMomani F, Khraisheh M. A decade of ceria based solar thermochemical H_2O/CO_2 splitting cycle. Int J Hydrogen Energy 2019;44(1):34–60. https://doi.org/10.1016/j.ijhydene.2018.04.080.
[26] Zainon AN, Somalu MR, Kamarul Bahrain AM, Muchtar A, Baharuddin NA, S A MA, Osman N, Samat AA, Azad AK, Brandon NP. Challenges in using perovskite-based anode materials for solid oxide fuel cells with various fuels: a review. Int J Hydrogen Energy 2023. https://doi.org/10.1016/j.ijhydene.2022.12.192. In press.
[27] Orfila M, Linares M, Pérez A, Barras-García I, Molina R, Marugán J, Botas JA, Sanz R. Experimental evaluation and energy analysis of a two-step water splitting thermochemical cycle for solar hydrogen production based on $La_{0.8}Sr_{0.2}CoO_{3-\delta}$ perovskite. Int J Hydrogen Energy 2022;47(97):41209–22. https://doi.org/10.1016/j.ijhydene.2022.03.077.
[28] Bu C, Gu T, Cen S, Liu D, Meng J, Liu C, Wang X, Xie H, Zhang J, Piao G. Reactivity and stability of Zr-doped CeO_2 for solar thermochemical H_2O splitting in combination with partial oxidation of methane via isothermal cycles. Int J Hydrogen Energy 2023;48(33):12227–39. https://doi.org/10.1016/j.ijhydene.2022.11.232.
[29] Gager E, Frye M, McCord D, Scheffe J, Nino JC. Reticulated porous lanthanum strontium manganite structures for solar thermochemical hydrogen production. Int J Hydrogen Energy 2022;47(73):31152–64. https://doi.org/10.1016/j.ijhydene.2022.07.052.
[30] Žužić A, Ressler A, Macan J. Perovskite oxides as active materials in novel alternatives to well-known technologies: a review. Ceram Int 2022;48(19):27240–61. https://doi.org/10.1016/j.ceramint.2022.06.152.
[31] Haeussler A, Abanades S, Jouannaux J, Julbe A. Non-stoichiometric redox active perovskite materials for solar thermochemical fuel production: a review. Catalysts 2018;8(12):611. https://doi.org/10.3390/catal8120611. article number.
[32] Orfila M, Linares M, Molina R, Botas JA, Sanz R, Marugán J. Perovskite materials for hydrogen production by thermochemical water splitting. Int J Hydrogen Energy 2016;41(42):19329–38. https://doi.org/10.1016/j.ijhydene.2016.07.041.
[33] Qian X, He JJ, Mastronardo E, Baldasarri B, Yuan W, Wolverton C, Haile SM. Outstanding properties and performance of $CaTi_{0.5}Mn_{0.5}O_{3-\delta}$ for solar-driven thermochemical hydrogen production. Matter 2021;4(2):688–708. https://doi.org/10.1016/j.matt.2020.11.016.
[34] Jin J, Fu M, Wang L, Ma T, Li X, Jin F, Lu Y. Water-splitting mechanism analysis of Sr/Ca doped $LaFeO_3$ towards commercial efficiency of solar thermochemical H_2 production. Int J Hydrogen Energy 2021;46(2):1634–41. https://doi.org/10.1016/j-ijhydene.2020.10.033.
[35] Lee E-S. Physical and chemical properties of $(Sr,Mg)FeO_{3-y}$ system heat-treated in N_2. Journal of the Korean Institute of Electrical and Electronic Material Engineers 2015;28(10):642–7. https://doi.org/10.4313/jkem.2015.28.10.642.
[36] Bertoldi J, de Campos Roseno KT, Schmal M, Lage VD, GonÇalves Lenzi G, Brackmann R. $La_{1-x}(Ce,Sr)_xNiO_3$ perovskite-type oxides as catalyst precursor to syngas production through tri-reforming of methane. Int J Hydrogen Energy 2022;47(72):31279–94. https://doi.org/10.1016/j.ijhydene.2022.07.053.
[37] Azcondo MT, Orfila M, Marugán J, Sanz R, Muñoz-Noval A, Salas-Colera E, Ritter C, García-Alvarado F, Amador U. Novel perovskite materials for thermal water splitting at moderate temperature. ChemSusChem 2019;12(17):4029–37. https://doi.org/10.1002/cssc.201901484.
[38] Azcondo MT, Orfila M, Linares M, Molina R, Marugán J, Amador U, Boulahya K, Botas JA, Sanz R. Thermochemical energy storage using the phase transitions brownmillerite -2H perovskite - cubic perovskite in the $Ca_xSr_{1-x}CoO_{3-\delta}$ (x = 0 and 0.5) system. ACS Appl Energy Mater 2021;4(8):7870–81. https://doi.org/10.1021/acsaem.1c01235.
[39] Pérez A, Orfila M, Linares M, Sanz R, Marugán J, Molina R, Botas JA. Hydrogen production by thermochemical water splitting with $La_{0.8}Al_{0.2}MeO_{3-\delta}$ (Me= Fe, Co, Ni and Cu) perovskites prepared under controlled pH. Catal Today 2022;390–391:22–33. https://doi.org/10.1016/j.cattod.2021.12.014.
[40] Gerasimov E, Kulikovskaya N, Chuvilin A, Isupova L, Tsybulya S. Microstructural changes in $La_{1-x}Ca_xCoO_{3-\delta}$ solid solutions under the influence of catalytic reaction of methane combustion. Top Catal 2016;59(15):1354–60. https://doi.org/10.1007/s11244-016-0661-4.
[41] Wang L, Al-Mamun M, Liu P, Wang Y, Yang HG, Zhao H. Notable hydrogen production on $La_xCa_{1-x}CoO_3$ perovskites via two-step thermochemical water splitting. J Mater Sci 2018;53(9):6796–806. https://doi.org/10.1007/s10853-018-2004-2.
[42] Murai K-I, Kori S, Nakai S, Moriga T. Effect of thermoelectric material of Ca or Fe-doped $LaCoO_3$. Int J Mod Phys B 2018;32(19):1840037. https://doi.org/10.1142/S0217979218400374. article number.
[43] Gálvez ME, Jacot R, Scheffe J, Cooper T, Patzke G, Steinfeld A. Physico-chemical changes in Ca, Sr and Al-doped La–Mn–O perovskites upon thermochemical splitting of CO_2 via redox cycling. P.C.C.P. 2015;17(9):6629–34. https://doi.org/10.1039/C4CP05898D.
[44] Meredig B, Wolverton C. First-principles thermodynamic framework for the evaluation of thermochemical H_2O or CO_2 splitting materials. Phys Rev B 2009;80(24):245119. https://doi.org/10.1103/PhysRevB.80.245119. article number.
[45] Muhich CL, Evanko BW, Weston C, Lichty P, Liang X, Martinek J, Musgrave CB, Weimer AW. Efficient generation of H_2 by splitting water with an isothermal redox cycle. Science 2013;341(6145):540–2. https://doi.org/10.1126/science.1239454.
[46] Hoskins AL, Millican SL, Czernik CE, Alshankiti I, Netter JC, Wendelin TJ, Musgrave CB, Weimer AW. Continuous on-sun solar thermochemical hydrogen production via an isothermal redox cycle. Appl Energy 2019;249:368–76. https://doi.org/10.1016/j.apenergy.2019.04.169.
[47] Merchán RP, Santos MJ, Medina A, Calvo Hernández A. High temperature central tower plants for concentrated solar power: 2021 overview", vol. 155. Renewable Sustainable Energy Rev.; 2022. p. 111828. https://doi.org/10.1016/j.reser.2021.111828. article number.
[48] Riaz A, Kremer F, Kim T, Sattayaporn S, Tsuzuki T, Lipinski W, Lowe A. Experimental demonstration of vanadium-doped nanostructured ceria for enhanced solar thermochemical syngas production. Nano Energy 2021;81:105639. https://doi.org/10.1016/j.nanoen.2020.105639. article number.
[49] Khamhangdatepon T, Sornchamni T, Siri-Nguan N, Laosiripojana N, Hartley UW. A dual reactor for isothermal thermochemical cycles of H_2O/CO_2 co-splitting using $La_{0.3}Sr_{0.7}Co_{0.7}Fe_{0.3}O_3$ as an oxygen carrier. Processes 2021;9(6):1018. https://doi.org/10.3390/pr9061018. article number.

Please cite this article as: Pérez A et al., Hydrogen production by isothermal thermochemical cycles using $La_{0.8}Ca_{0.2}MeO_{3\pm\delta}$ (Me = Co, Ni, Fe and Cu) perovskites, International Journal of Hydrogen Energy, https://doi.org/10.1016/j.ijhydene.2023.06.272

[50] Danks AE, Hall SR, Schnepp Z. The evolution of 'sol-gel' chemistry as a technique for materials synthesis. Mater Horiz 2016;3(2):91–112. https://doi.org/10.1039/c5mh00260e.
[51] Orfila M, Linares M, Molina R, Marugán J, Botas JA, Sanz R. Hydrogen production by water splitting with $Mn_{3-x}Co_xO_4$ mixed oxides thermochemical cycles: a thermodynamic analysis. Energy Convers Manag 2020;216:112945. https://doi.org/10.1016/j.enconman.2020.112945. article number.
[52] Orfila M, Sanz D, Linares M, Molina R, Sanz R, Marugán J, Botas JA. H_2 production by thermochemical water splitting with reticulated porous structures of ceria-based mixed oxide materials. Int J Hydrogen Energy 2021;46(33):17458–71. https://doi.org/10.1016/j.ijhydene.2020.04.222.
[53] Leitner J, Chuchvalec P, Sedmidubský D, Strejc A, Abrman P. Estimation of heat capacities of solid mixed oxides. Thermochim Acta 2003;395(1–2):27–46. https://doi.org/10.1016/S0040-6031(02)00177-6.
[54] Scheffe JR, Weibel D, Steinfeld A. Lanthanum–Strontium–Manganese perovskites as redox materials for solar thermochemical splitting of H_2O and CO_2. Energy Fuels 2013;27(8):4250–7. https://doi.org/10.1021/ef301923h.
[55] Aguadero A, Falcon H, Campos-Martin JM, Al-Zahrani SM, Fierro JLG, Alonso JA. An oxygen-deficient perovskite as selective catalyst in the oxidation of alkyl benzenes. Angew Chem 2011;50(29):6557–61. https://doi.org/10.1002/anie.201007941.
[56] Li S, Irvine JTS. Non-stoichiometry, structure and properties of proton-conducting perovskite oxides. Solid State Ionics 2021;361:115571. https://doi.org/10.1016/j.ssi.2021.115571. February, article number.
[57] Ethiraj AS, Kang DJ. Synthesis and characterization of CuO nanowires by a simple wet chemical method. Nanoscale Res Lett 2012;7(1):70. https://doi.org/10.1186/1556-276X-7-70. article number.
[58] Sastre D, Carrillo AJ, Serrano DP, Pizarro P, Coronado JM. Exploring the redox behavior of $La_{0.6}Sr_{0.4}Mn_{1-x}Al_xO_3$ perovskites for CO_2-splitting in thermochemical cycles. Top Catal 2017;60(15–16):1108–18. https://doi.org/10.1007/s11244-017-0790-4.
[59] Ran R, Wu X, Weng D, Fan J. Oxygen storage capacity and structural properties of Ni-doped $LaMnO_3$ perovskites. J Alloys Compd 2013;577:288–94. https://doi.org/10.1016/j.jallcom.2013.05.041.
[60] Cihlar J, Vrba R, Castkova K, Cihlar J. Effect of transition metal on stability and activity of La-Ca-M-(Al)-O (M = Co, Cr, Fe and Mn) perovskite oxides during partial oxidation of methane. Int J Hydrogen Energy 2017;42(31):19920–34. https://doi.org/10.1016/j.ijhydene.2017.06.075.
[61] Tarjomannejad A, Niaei A, Farzi A, Salari D, Zonouz PR. Catalytic oxidation of CO over $LaMn_{1-x}B_xO_3$ (B = Cu, Fe) perovskite-type oxides. Catal Lett 2016;146(8):1544–51. https://doi.org/10.1007/s10562-016-1788-4.
[62] Marugán J, Botas JA, Martín M, Molina R, Herradón C. Study of the first step of the Mn_2O_3/MnO thermochemical cycle for solar hydrogen production. Int J Hydrogen Energy 2012;37(8):7017–25. https://doi.org/10.1016/j.ijhydene.2011.10.124.
[63] Herradón C, Molina R, Marugán J, Botas JA. Experimental assessment of the cyclability of the Mn_2O_3/MnO thermochemical cycle for solar hydrogen production. Int J Hydrogen Energy Jan. 2019;44(1):91–100. https://doi.org/10.1016/J.IJHYDENE.2018.06.158.
[64] Orfila M, Linares M, Molina R, Botas JA, Marugán J, Sanz R. Thermochemical hydrogen production using manganese cobalt spinels as redox materials. Int J Hydrogen Energy 2017;42(19):13532–43. https://doi.org/10.1016/j.ijhydene.2017.02.027.
[65] Bekru AG, Zelekew OA, Andoshe DM, Sabir FK, Eswaramoorthy R. Microwave-assisted synthesis of CuO nanoparticles using *Cordia africana* lam. Leaf extract for 4-nitrophenol reduction. J. Nanotechnol. 2021;2021:5581621. https://doi.org/10.1155/2021/5581621. article number.
[66] Ma T, Wang L, Chang C, Akhatov JS, Fu M, Li X. A comparative thermodynamic analysis of isothermal and non-isothermal CeO_2-based solar thermochemical cycle with methane-driven reduction. Renew Energy 2019;143:915–21. https://doi.org/10.1016/j.renene.2019.05.047.

Please cite this article as: Pérez A et al., Hydrogen production by isothermal thermochemical cycles using $La_{0.8}Ca_{0.2}MeO_{3\pm\delta}$ (Me = Co, Ni, Fe and Cu) perovskites, International Journal of Hydrogen Energy, https://doi.org/10.1016/j.ijhydene.2023.06.272